Polymer 50 (2009) 1470–1482

Contents lists available at ScienceDirect

Polymer

journal homepage: www.elsevier.com/locate/polymer

Determination of eugenol diffusion through LLDPE using FTIR-ATR flow cell and HPLC techniques

G. Dhoot [a], R. Auras [a,*], M. Rubino [a], K. Dolan [b], H. Soto-Valdez [c]

[a] School of Packaging, Michigan State University, East Lansing, MI 48824-1223, United States
[b] Biosystems and Agricultural Engineering, Michigan State University, East Lansing, MI 48824-1223, United States
[c] Centro de Investigación en Alimentación y Desarrollo, A.C., Hermosillo, Sonora 83000, México

ARTICLE INFO

Article history:
Received 22 October 2008
Received in revised form
7 January 2009
Accepted 10 January 2009
Available online 15 January 2009

Keywords:
Eugenol
LLDPE
FTIR-ATR

ABSTRACT

A time-resolved Fourier Transform Infrared-Attenuated Total Reflectance Spectroscopy (FTIR-ATR) technique was set up and used to study the diffusion of eugenol through Linear Low Density Polyethylene (LLDPE) at 16, 23 and 40 °C. The 1514 cm^{-1} peak for eugenol (aromatic –C═C– stretching) was monitored over time and used to determine the diffusion coefficient (D). The Fickian model was found to fit well to the experimental data and the D value of eugenol through LLDPE was found to be between 1.05 ± 0.01 and $13.23 \pm 0.18 \times 10^{-10}$ cm^2/s. The FTIR-ATR results were compared with one and two side diffusion process using a permeation cell and quantified by High Performance Liquid Chromatography (HPLC) technique. Eugenol sorbed in LLDPE samples at different times, was extracted in methanol and the concentration determined by HPLC. The diffusion coefficient by both two-sided and one-sided HPLC technique was found to be approximately three times higher than the FTIR-ATR values although they were in the same order of magnitude of 10^{-10} cm^2/s. The difference between the FTIR-ATR and HPLC results was mainly attributed to difference between the two measuring techniques.

1. Introduction

The diffusion coefficient (D) of permeants through polymeric materials is one of the main kinetic parameters used to evaluate barrier properties and performance of membranes in applications areas such as chemical and environmental engineering, food science, medicine, and packaging. In general, D is determined by variations of isostatic and quasi isostatic techniques, which have been developed to study the diffusion processes. Based on the type of permeants, for non-condensable gases detection methods like chromatography (GC) or high performance liquid chromatography (HPLC) are used and for condensable gases gravimetric techniques are used [1]. Many other techniques, like those based on inverse gas chromatography using capillary columns [2], nuclear magnetic resonance (NMR) spectroscopy [3], proton-induced X-ray emission (PIXE) or proton-induced gamma-ray emission (PIGE) have also been explored [4]. The use of Infrared (IR) spectroscopy in various modes like transmission Fourier transform spectroscopy (FTIR) [5], FTIR imaging [6] and FTIR-ATR (attenuated total internal reflectance) imaging [7], and FTIR-ATR spectroscopy [8–28] for diffusion analysis, has also been widely studied by many research groups.

FTIR-ATR system has various advantages over other conventional immersion techniques, in which the polymer sample is first immersed in the permeant (in case of liquids) for different periods of time, and then the permeant sorbed in the polymer is quantified by weight or concentration changes in a gravimetric instrument or by chromatography, respectively. Unlike in these techniques, with FTIR-ATR, it is possible to monitor the mass transfer throughout the process until the equilibrium condition is reached. In addition, the permeant and polymer chemical interactions can be monitored [9,21,25], and the change in polymer conformational regularity [29], crystallinity [9] and swelling can be observed as the mass transfer proceeds [9,26]. Balik and Simendinger, Elabd et al., and Murphy et al., used this technique successfully for determining the D values in multi-component systems [8,10,20]. Esmaiel and Peppas studied the case of polymer–polymer inter-diffusion [11], and Hace et al. used this technique for monomer–polymer diffusion determination [27]. In the medical field, FTIR-ATR technique has been valuable for determining controlled release of drugs from suspensions [15]. Also, the low penetration depth of attenuated infrared radiation has helped determining the mass transfer in ultrathin films [16] and polymer membranes [20,23].

* Corresponding author. School of Packaging, Michigan State University, East Lansing, 140 Packaging Building, MI 48824-1223, United States. Tel.: +1 517 432 3254; fax: +1 517 353 8999.
E-mail address: aurasraf@msu.edu (R. Auras).

0032-3861/$ – see front matter © 2009 Elsevier Ltd. All rights reserved.
doi:10.1016/j.polymer.2009.01.026

In earlier studies involving FTIR-ATR, most of the systems consisted of a polymer film sandwiched between a stationary permeant reservoir and an ATR crystal. In these cases, optimum contact between the polymer film and the crystal was ensured by solution or melt casting, or hot pressing the film over the crystal. However, this meant that the morphological properties of such a film would be different from commercially available film, and hence it would be difficult to correlate their mass transfer properties. Another problem was the possibility of loss of contact between the film and the crystal in cases where the permeant would cause swelling in the film [8]. To overcome this problem, many groups used the flow pressure of gas or liquid permeant over the polymer film to ensure good contact with the ATR crystal [8,20,28,29], although the experimental conditions to obtain proper contact and successful fitting of the experimental data are not always detailed and explained. Very few researchers like Yi et al., have actually evaluated the change in diffusion coefficient caused by change in permeant flow pressure [28]. Until now most studies involved polymer/permeant systems with distinct IR absorbance peaks. These however restrict the choice of polymer/permeant system that can be analyzed using this technique.

HPLC has long been used in migration analysis of different polymers to determine diffusion coefficients of non-condensable gases such as butylated hydroxyl toluene (BTH) [1], phthalates [30], and 1,4-diphenyl-1,3-butadiene [31]. This type of study seeks to determine the rate of release of chemical compounds into different liquid phase simulants like water, ethanol or oil. If the compatibility between the chemical compound and the liquid phase is high, the rate of release increases and so does the diffusion coefficient. Balik et al. have shown a mismatch between the diffusion coefficient obtained by the FTIR-ATR and gravimetric measurement techniques [8]. Even though HPLC and FTIR-ATR are widely used to determine the diffusion coefficient of chemical compounds in polymers, to the authors' best knowledge no study has compared the diffusion coefficients obtained between them.

In this paper, the setup of a time-resolved FTIR-ATR technique is outlined and used to study the diffusion process in a system where distinct polymer/permeant IR absorbance peaks could not be obtained. Eugenol, a natural complex organic compound with antioxidant and antimicrobial properties, mainly extracted from cloves was chosen as the permeant and Linear Low Density Polyethylene (LLDPE) as the polymer [32,33]. Eugenol has shown great potential for use in food packaging applications [34]. Understanding the diffusion of eugenol through LLDPE is of interest for developing antimicrobial and antioxidant films. So, diffusion of eugenol through LLDPE was studied at 16, 23 and 40 °C. D was determined by continuously monitoring the eugenol absorbance peak. The system was first analyzed at different conditions of eugenol flow rates and penetration angle of the IR radiation. The FTIR-ATR results were then compared with one and two-sided diffusion permeation process using a permeation cell and quantified by HPLC technique.

2. FTIR-ATR diffusion analysis theory

When passed through an ATR crystal IR radiation undergoes total internal reflection at the interface between the high refractive index crystal and low refractive index medium present at the top of the crystal. The IR ray reflects multiple times in the crystal giving rise to an evanescent field of radiation at the interface which penetrates inside the medium. The evanescent field strength is strongest at the interface and decreases exponentially as its depth in the rarer medium increases (Equation (1)).

$$\frac{E}{E_o} = e^{-\gamma z} \tag{1}$$

where E/E_o is the relative loss in the electric field strength compared to its value at the interface, γ is the reciprocal of the depth of penetration or evanescent wave decay coefficient and z is the distance in the rarer medium from the crystal surface. Historically, the depth at which the evanescent field strength reduces to 37% its strength at the interface has been called the depth of penetration d_p. However, the actual depth of penetration is higher and almost three times d_p. But in case of polymers and organic compounds which are weakly IR-absorbing, sampling depth experiments have shown that depth of penetration can be accepted to be given by d_p in Equation (2) [35].

$$d_p = \frac{1}{\gamma} \tag{2}$$

where

$$\gamma = \frac{2n_2\pi\sqrt{\sin^2\theta - \left(\frac{n_1}{n_2}\right)^2}}{\lambda} \tag{3}$$

where n_1 and n_2 represent the refractive indices of dense (ATR crystal) and rarer medium (polymer), λ is the wavelength and θ is the angle of penetration of incident radiation.

In a typical diffusion experiment, the IR-absorbing permeant is placed over the film, which is in contact with the ATR crystal. The permeant diffuses through the film and is detected when it reaches the profiling depth d_p in the film. A time-resolved study of the characteristics IR peaks of the permeant helps monitor and study the entire diffusion process. In this case, it is assumed that the refractive index of the polymer film is same at all wavenumbers and that the permeant diffusion does not create any change in the refractive index. However, since we have total internal reflection in ATR spectroscopy, the absorption peak is influenced not only by the extinction coefficient (k) but also the refractive index (n), giving rise to the more complex refractive index n' (Equation (4)). Huang et al., studied the ATR spectrum of polyethylene by performing Kramers–Kronig transformation (KKT) and Fresnel reflectivity analysis and found difference in the peak intensity ratio of the 720 and 730 cm^{-1} peaks in the ATR spectrum and the true spectrum obtained after the transformation [36]. A technique called peak ratioing is generally performed in ATR diffusion study at each stage of the diffusion process by ratioing the permeant absorbance peak to the corresponding polymer absorbance peak. This helps to account for any changes in the polymer film, like swelling and also changes in polymer/crystal contact [8]. However, the study by Huang et al. [36] shows that the constant refractive index assumption during peak ratioing, especially when the peak separation gap between the permeant and polymer peaks is high, may need reconsideration, because refractive index changes with change in wavenumber.

$$n' = n(1 + ik) \tag{4}$$

The Beer–Lambert law (Equation (5)) helps relate the IR absorbance values of the polymeric sample to its concentration. This law however, is mostly applicable for weakly absorbing species. Mirabella [37], studied the absorption coefficient (α) for polypropylene and found it to be $\leq 10^4$, which falls in the range of weakly absorbing material. Hence, this law for weakly IR-absorbing species holds true in most organic materials like polymers.

$$A = \int_0^L eCE_o^2 \exp(-2\gamma z)dz \tag{5}$$

where e is the molar extinction coefficient and C is the concentration of absorbing sample. Based on the boundary conditions for diffusion through a plane sheet (Equations (6–8)) given by Crank

[36], (Equation (9)), and by solving Equation (5) simultaneously with 1–3, the calculation of the diffusion coefficient of a permeant through a polymeric material can be determined by solving Equation (10) [14].

$$C = C_0 \text{ at } t = 0 \text{ and } 0 < z < L \tag{6}$$

$$C = C_1 \text{ at } t \geq 0 \text{ and } z = L \tag{7}$$

$$\frac{\partial C}{\partial z} = 0 \text{ at } t \geq 0 \text{ and } z = 0 \tag{8}$$

where $z = L$ accounts for the interface between the solute and the polymer, and $z = 0$ accounts for the interface between the ATR crystal and the polymer.

$$\frac{\partial C}{\partial t} = D\frac{\partial^2 C}{\partial z^2} \tag{9}$$

where C is the concentration of the permeant, t is the time, z is the direction of diffusion in the polymer and D is the concentration independent diffusion coefficient.

$$\frac{A_t}{A_{\text{eqb}}} = 1 - \frac{8\gamma}{\pi(1-\exp(-2\gamma l))}\sum_{n=0}^{\infty}\frac{\exp(g)\left[(-1)^n 2\gamma + f\exp(-2\gamma l)\right]}{(2n+1)\left(4\gamma^2 + f^2\right)} \tag{10}$$

where

$$g = \frac{-D(2n+1)^2\pi^2 t}{4l^2} \quad f = \frac{(2n+1)\pi}{2l}$$

where A_t and A_{eqb} are the normalized absorbance values at time t and equilibrium respectively, and l is the thickness of the polymer.

The D can be found by fitting the experimental absorbance data with Equation (10). A predicted or theoretical diffusion curve can be obtained based on parameters as polymer and ATR crystal refractive indices, wavelength of the permeant peak studied, polymer thickness, and time. The best fit between the experimental absorbance value and the predicted fit can be determined by analyzing the sum of squared errors, and the D value corresponding to the least error is taken to be the best fit [14].

3. Materials and methods

3.1. Materials

The commercial polymer film used in this study was LLDPE film ($n_1 = 1.5$, thickness $L = 25 \pm 4$ μm, obtained from Flexopak, Attiki, Greece). The permeant used in this study was eugenol (≥98% from Sigma–Aldrich, St. Louis, MO, USA). LLDPE was chosen because it is one of the most commonly used food contact polymer, and also the simple spectrum of LLDPE provides a wide region for detecting the permeant IR absorbance peak. Fig. 1 shows the chemical structure for eugenol and the constitutional unit of LLDPE.

3.2. Methods

3.2.1. FTIR-ATR flow cell setup

A Shimadzu IR Prestige-21 spectrophotometer from Shimadzu Scientific Instruments (Columbia, MD, USA) with an attenuated total reflection accessory ATR MAX II and a liquid jacketed flow cell assembly from Pike Technologies (Madison, WI, USA) were used. A $56 \times 10 \times 4$ mm ZnSe crystal ($n_2 = 2.43$) from Pike Technologies was used with the ATR accessory. Fig. 2 shows the ATR cell design used in this study. The cell is mainly divided into two parts. The top

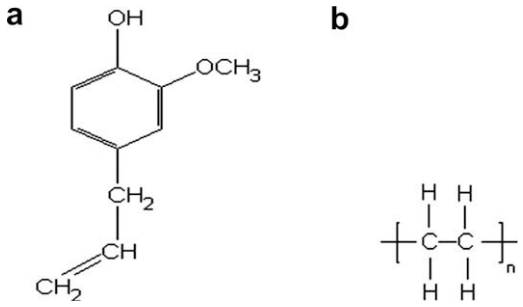

Fig. 1. Chemical structure (a) Eugenol and (b) LLDPE.

part provides the eugenol inlet and outlet, and also includes a water jacket for cell temperature control. The bottom half consists of the LLDPE film, which is placed on the ATR crystal and sealed in place with an O-ring and Aluminum laminated plastic support. The two halves are then screwed together, and the seal is achieved with the help of an outer O-ring. Fig. 3 shows the entire flow circuit. Insulated platinum cured silicone tubing and a Masterflex C/L pump from Cole Parmer Instrument Company (Vernon Hills, IL, USA) were used to pump eugenol at three different flow rates of 6, 8 and 11 ml/min. A small glass tube was used to connect the tubing with the flow cell inlet and outlet. A 5 l water bath (Neslab Instruments Inc., Newington, NH, USA) was used for controlling the temperature of eugenol and the flow cell. A thermocouple at the outlet of the flow cell was used to continuously monitor eugenol temperature. To maintain the temperature of liquid eugenol in the reservoir constant, an outer loop was created by using two 3-way ball valves. Temperature controls for the cell and eugenol were achieved with precisions higher than ±0.5 °C. A study was performed to determine the D value at "no flow" or 0 ml/min condition. In this case, one side of the LLDPE film was heated on a hot plate at 50 °C for 30 s and then placed on the ATR crystal. Eugenol was then injected into the closed cell.

The FTIR-ATR experiment was performed by first taking the background scan of air and then placing the sample in the flow cell for 30 min to equilibrate with the cell temperature. Then 30 infrared scans at every 2 min and 4 cm^{-1} resolution were taken to obtain the absorbance data at 45° or 39° incident angles. Fig. 4 shows that all LLDPE characteristics peaks were overlapped by eugenol peaks, and even de-convolution of these overlapped peaks did not enable isolation of the LLDPE peak. Table 1 shows the main absorption peaks of LLDPE and eugenol and their functional group assignments. Trial runs showed that a sharp peak at 1514 cm^{-1} (aromatic –C═C– stretching) in eugenol gave consistent results for the diffusion analysis study, and hence the change in absorbance ($A_{t=t} - A_{t=0}$) of this peak, measured by change in peak height, was studied over time for this experiment. Trial runs were conducted to determine the amount of time needed to reach steady state of mass transfer. Steady state was considered when the absorbance values deviated by less than 1% over time period of 30 min. A small constant increase in the absorbance value of the eugenol peak, during the steady state was observed as eugenol permeated through the film and settled over the crystal. Hence, exact equilibrium absorbance value was actually found by fitting the theoretical curve from Equation (10) and finding the best value of equilibrium absorbance by regression. Each absorbance value was then normalized by dividing it by the absorbance at equilibrium, and compared with theoretical curve from Equation (10) to get D value.

Although the refractive index of the substrate in the absorbing region of the spectrum, in ATR spectroscopy undergoes a complex change [35], like many other earlier studies using this technique

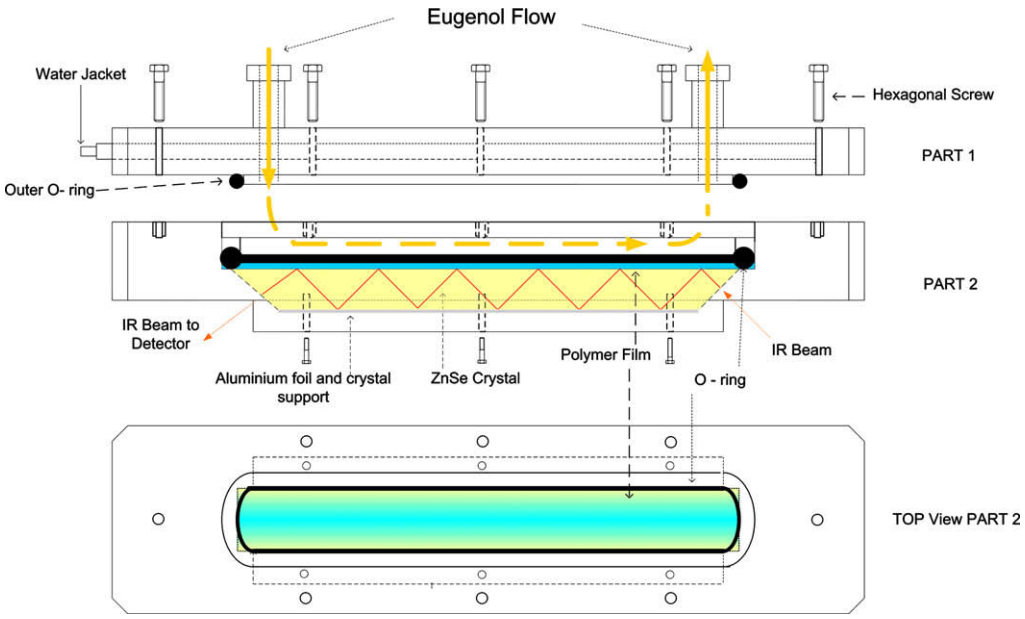

Fig. 2. FTIR-ATR flow cell design (adapted from Pike Technologies).

[8–13,17,21,24–28], we assumed constant refractive index at the 1514 cm^{-1} peak. Since peak ratioing could not be performed, we had to assume constant refractive index only at one absorption peak (1514 cm^{-1}), thus reducing the error that would have been involved with monitoring of two peaks (polymer and penetrant) separated by some wavenumber range. However, inability to measure polymer peak meant we could not monitor the changes in polymer/crystal contact and had to rely on the eugenol flow pressure to achieve optimum contact with the crystal. Also, it was assumed that the diffusing permeant (eugenol) did not cause any change in the refractive index of the polymer (LLDPE), and hence the depth of penetration of the IR radiation was constant. Since most organic compounds are considered as weakly IR-absorbing [35], eugenol may have caused zero or minimal change in the refractive index. This assumption may be valid also because no interaction was observed between eugenol and LLDPE through the diffusion process as established by the lack of chemical interaction or swelling of LLDPE which could lead to change in refractive index. All the experiments were performed in triplicates at temperatures of 16, 23 and 40 °C.

3.2.2. HPLC method

The results obtained from the FTIR-ATR experiment were compared to those from a more conventional diffusion technique using one-sided and two-sided permeation experiment, monitored by HPLC. Round samples (area 3.14 cm^2) were cut from the LLDPE film and placed in 40 ml vials containing 30 ml eugenol (Fig. 5a). The film samples were introduced in the vials and extracted at variable time intervals until equilibrium was reached at each temperature. Four replications were included in each vial. The experiment was performed at 16, 23, and 40 °C with maximum of 0.5 °C variation. After taking the film samples from the eugenol

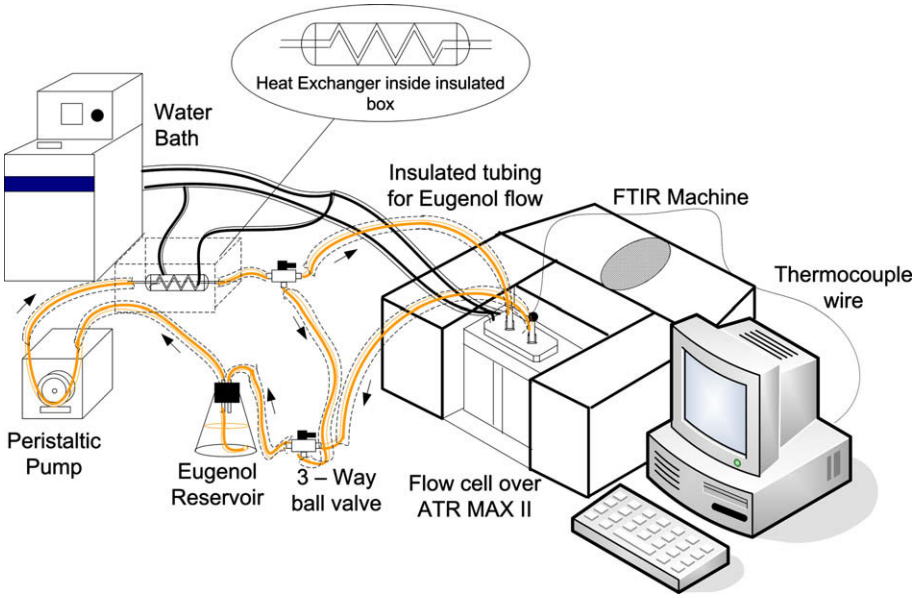

Fig. 3. FTIR-ATR experimental setup.

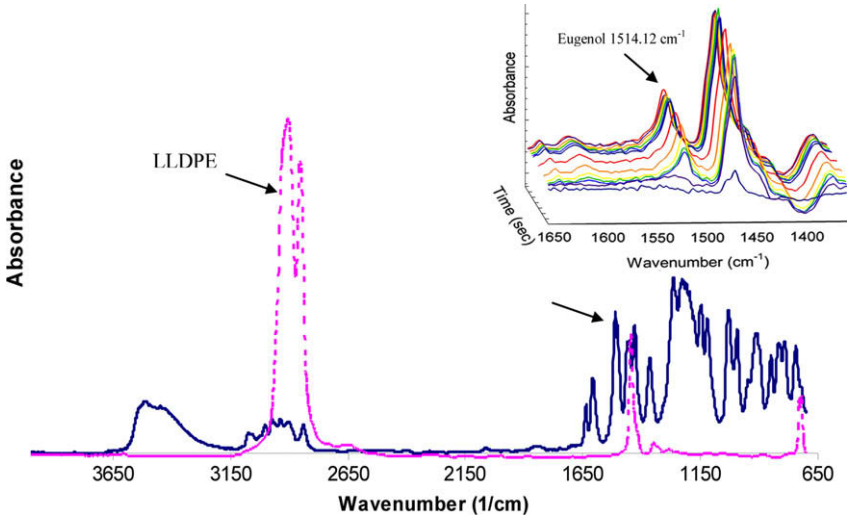

Fig. 4. Eugenol and LLDPE overlapped infrared spectrum. Dark line indicates the eugenol spectrum overlapped on light dotted line of LLDPE Spectrum. The figure in the top corner shows the increase in eugenol absorbance with increase in time.

vials, excess eugenol was first wiped off from the film surface. Then the films were immersed in 10 ml methanol (HPLC grade) for 10 s to ensure no eugenol was left on the film surface. Finally, each film sample was placed in 20 ml methanol and continuously stirred for 24 h at room temperature for eugenol extraction. In pilot trial runs by HPLC, we confirmed that 99.99% of the eugenol extraction took place within the first 24 h. An HPLC equipment (Waters 2695) coupled with a UV detector (Waters 2487) and equipped with a Nova-Pak® C18 (4 μm) column (all from Waters Corporation, MA, USA) at 25 °C were used to quantify eugenol. A 10 μl injection volume and an isocratic elution of 1 ml/min flow with methanol: water (85:15) was used. The data was collected at 280 nm and the retention time for eugenol was found to be 1.5 min. A calibration curve was generated by injecting eugenol standard (99% pure from Sigma Aldrich, MO, USA) solutions in methanol (0.43–10 μg/ml). The peak area response was collected in triplicates for each standard solution and a calibration curve of area response (A.U.) vs concentration (μg eugenol/ml methanol) was plotted ($R^2 = 0.9991$).

In one-sided HPLC experiment, LLDPE film was placed in the permeation cell built from Aluminum alloy 2024 with eugenol reservoir on just one side (Fig. 5). The entire assembly was sealed using Viton® O-Rings. The film area of 15.2 cm^2 was exposed to eugenol on one side. The other side was open to atmosphere. The film was taken out of the cell at variable time intervals until equilibrium was reached at each temperature. Excess eugenol on the film surface was wiped out. Four circular samples of 1.53 cm^2 were cut from the exposed film area and their surface cleaned in methanol (HPLC grade). The films were weighed and placed in 10 ml methanol for 24 h and at room temperature for extraction. The weight of eugenol extracted was subtracted from the film weight to finally normalize the amount of eugenol sorption per mg of the film sample. All other parameters for eugenol quantification were same as the two side HPLC experiment. These experiments were performed at 16, 23 and 40 °C with maximum of 0.5 °C variation.

Table 1
Main IR absorption peaks for LLDPE and eugenol.

Wavenumber cm^{-1}	Chemical functional groups	
Vibration mode	Eugenol	LLDPE
2870 (sym), 2960 (asym) stretching	Methyl ($-CH_3$)	–
1370 (sym), 1450 (asym) bending	Methyl ($-CH_3$)	Methyl ($-CH_3$)
2860 (sym), 2930 (asym) stretching	Methylene ($-CH_2-$)	Methylene ($-CH_2-$)
1465, 720 bending	Methylene ($-CH_2-$)	Methylene ($-CH_2-$)
3000, 3040 stretching	C=C>H	–
650–1000 bending	C=C<H	–
910, 990 bending	Vinyl $C{=}CH_2$	–
1514, 1608, 1637 stretching	Aromatic C=C	–
3300–3550 stretching	Phenol CO>H	–
1300–1400 bending	CO<H	–

The data obtained, was then tested to fit the Fick's model expressed by Equation (11), for sorption of permeant having constant D in plane sheet [38]. This diffusion model was used for the one and two side diffusion process.

$$\frac{M_t}{M_{eqb}} = 1 - \frac{8}{\pi^2}\sum_{n=0}^{\infty}\frac{1}{(2n+1)^2}\exp\left[\frac{-D(2n+1)^2\pi^2 t}{L^2}\right] \tag{11}$$

where M_t and M_{eqb} are concentration weight (μg of eugenol per mg LLDPE) of eugenol sorbed at time t and equilibrium, respectively. L is the polymer film thickness. In the case of one-sided sorption, L was replaced by $2L$, taking into account the change in boundary conditions.

3.2.3. Statistical analysis

The best overall fit D and M_∞ values for four replications for the HPLC runs, the best overall fit D and A_∞ values for three runs for the FTIR-ATR experiments, the prediction interval for the observed experimental values, and the confidence intervals for best fit values were calculated by using non-linear regression (nlinfit) function in MATLAB R2008 (MathWorks, Natick, MA, USA). Significant differences between the D values were determined by using Tukey's test. Calculations for least significance difference (LSD) were performed in Matlab using student's t distribution table [39].

Sensitivity coefficient helps determine the optimum range of times to estimate a parameter. The optimum time to estimate parameter D is the time where the sensitivity coefficient is maximized [40] The scaled sensitivity coefficient of D is the product of D and the derivative of the dependent variable with respect to D, and the derivative was evaluated numerically:

$$D\frac{\partial Y_i}{\partial D} \approx D\frac{Y_i(D+\delta D) - Y_i(D)}{\delta D} \tag{12}$$

where δD was a small value $= 0.000001D$, and $Y_i = A_t/A_{eqb}$ from Equation (10) or M_t/M_{eqb} from Equation (11). The scaled sensitivity coefficient of D was plotted vs time.

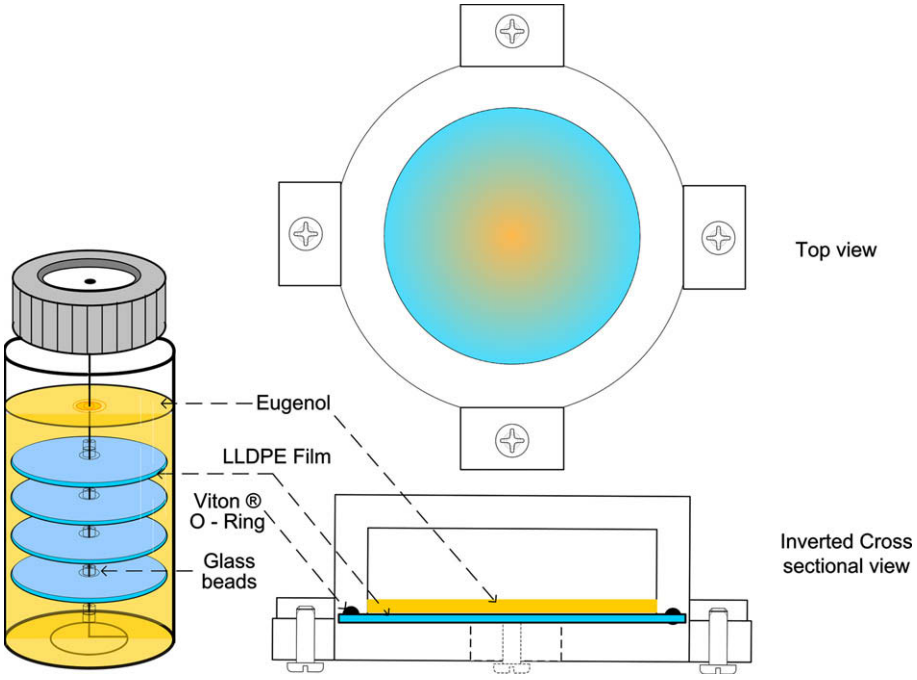

Fig. 5. HPLC based technique (a) Two side experiment vials (b) One side experiment permeation cell.

4. Results and discussion

The inset in Fig. 4 shows the increase in absorbance, observed in the eugenol peak (1514 cm^{-1}) and adjacent LLDPE peak (1462 cm^{-1}) over time. As mentioned earlier, eugenol has a complex structure (Fig. 1a), in which the main IR absorption peaks overlap the spectrum of LLDPE (Fig. 4 and Table 1). Hence, it was not possible to perform peak ratioing. Peak ratioing can act as internal standard during the experiment, but it restricts the type of polymer/permeant system that can be used in the experiment. Since peak rationing could not be used and the initial best flow conditions were not known at the beginning of the experiments, four different flow rates of 0, 6, 8 and 11 ml/min were run in triplicate to determine the optimum flow rate. Fig. 6 shows the normalized absorbance data for eugenol at 1514 cm^{-1} at 23 °C as fitted by Equation (10), and obtained at these four flow rates. The plots show the experimental values of normalized absorbance of all three-replication runs. The center line is the best predicted theoretical curve based on the Fickian model (Equation (10)). The 95% confidence interval lines are very close to the predicted best-fit curve, hence not clearly visible in Fig. 6. The outer lines indicate the 95% prediction interval of the observed values. The figures below show the corresponding standard residual errors between the experimental and predicted values. Values along the dark line i.e. zero residual, indicate exact match with the predicted values. Higher standard residuals, up to 4 standard residual, were observed at initial times (below 0.5×10^4 s or 1.4 h) under all the four flow conditions. However, the number of experimental data points with higher residuals was limited and hence does not truly affect the value of D, the details of which are addressed later. This initial residual may be due to the initial instability of the LLDPE film and crystal contact. After the initial part of diffusion process, the experimental values deviated uniformly by 2 standard residuals from the zero line, which can be considered as good fit. Table 2 shows the D values and the root mean square error (RMSE) involved in the measurements at the four flow rates. The values of D at 0, 6 and 8 ml/min are close at 2.45×10^{-10}, 2.91×10^{-10} and 3.37×10^{-10} cm^2/s respectively, while the D at 11 ml/min is 4.90×10^{-10} cm^2/s. The transport of the permeant across the polymer film doest not depend only on diffusive transport but also on bulk flow induced by the pressure of the permeant flow system. However, bulk flow becomes a predominant mechanism in case of high degree of membrane swelling [41]. Hence, as we did not observe any swelling in the polymer film, bulk flow might not be the significant factor responsible for the rise in D with flow rate. One reason for the increase in D may be due to the faster increase in the absorbance due to more rapid achievement of efficient contact between the film and the crystal, which could not be accounted for by performing peak ratioing. Hence, the best flow rate was decided on the basis of RMSE values. The error values decreased with increased flow rate up to 8 ml/min, but were higher at 11 ml/min possibly due to some instability in film contact that may have occurred at high flow rate due to higher turbulence in the flow cell. Hence, all further experiments were performed at 8 ml/min.

Further studies were carried out at an angle of penetration of 39°, to determine if the increase in IR penetration depth could minimize the initial errors. Fig. 7 shows the normalized increase in eugenol absorbance with increase over time at 45° and 39° angle of penetration, respectively. Increasing depth of penetration (i.e. lower angle) meant getting close to the critical angle (~37° based on constant refractive index assumption). As seen in Fig. 7, highly variable data was obtained at 39°, which may have been the result of the spectrum distortion. As we approach the critical angle, the depth of penetration becomes indefinitely large, and the electric field amplitude changes abruptly, thus distorting the spectrum [35]. Table 3 shows the D and the error involved in the experimental and predicted values at the two angles. Since the 45° incident angle resulted in lower RMSE, all experiments were performed at 45°.

The normalized eugenol absorbance over time at three different temperatures 16, 23 and 40 °C is shown in Fig. 8. The increase of eugenol absorbance at 40 °C was much faster than at 23 and 16 °C, taking only 1×10^4 s (2.8 h) to reach steady state. Higher residuals at the initial times can be seen in the plot of standard residuals for

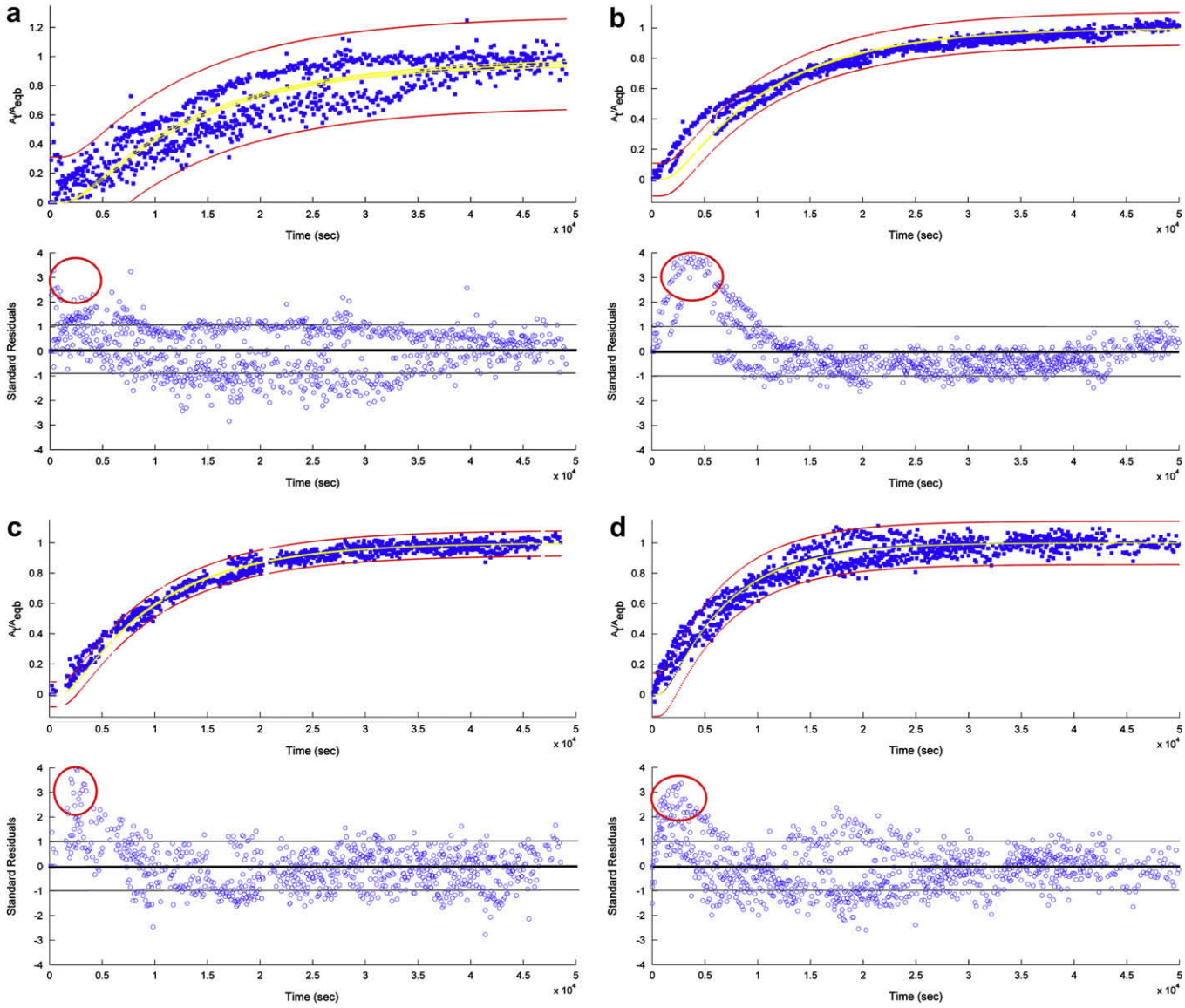

Fig. 6. FTIR-ATR normalized eugenol (1514 cm^{-1}) absorbance vs time for 23 °C at three flow rates, (a) 0 ml/min, (b) 6 ml/min, (c) 8 ml/min and (d) 11 ml/min. The central line shows the best fit to the dotted experimental values of all the three replications. The outer lines show the prediction interval for the observed experimental values. The confidence interval of the best fit is very close to the fitted curve and not clearly visible in the figures. The standard residuals are shown in the graphs below with dark line indicating zero residual. The red oval indicates the higher residuals. (For interpretation of the references to colour in this figure legend, the reader is referred to the web version of this article.)

all the three temperatures, which could be mainly due to the inefficient contact between the LLDPE film and the crystal. In order to determine the effect of lack of fit of initial higher residuals, the experimental data were fitted by replacing the initial absorbance data by the best-predicted values. Despite the perfect fit of the initial data, this procedure did not significantly change the D values. D with perfect initial fit was 3.32×10^{-10} cm^2/s compared to D without discarding the initial data of 3.37×10^{-10} cm^2/s obtained at 23 °C. Moreover, after running the sensitivity of D in Equation (10) and plotting against time, the value of D was most sensitive (highest point of sensitivity curve) in the region of $0.4 < A_t/A_{eqb} < 0.6$, where the theoretical diffusion curve fits well with the experimental values (Fig. 9). Hence, the higher residuals in the initial stage did not significantly affect the results for D.

Figs. 10 and 11 show the normalized mass gain at three temperatures (16, 23 and 40 °C) obtained by two-sided and one-

Table 2
Diffusion coefficient (D) and error by FTIR-ATR at different eugenol flow rates and at 23 °C.

0 ml/min		6 ml/min		8 ml/min		11 ml/min	
$D \times 10^{-10}$ [a] (cm^2/s)	RMSE	$D \times 10^{-10}$ [a] (cm^2/s)	RMSE	$D \times 10^{-10}$ [a] (cm^2/s)	RMSE	$D \times 10^{-10}$ [a] (cm^2/s)	RMSE
$2.45 \pm 0.05_a$ (2.34–2.56)	0.1266	$2.91 \pm 0.02_b$ (2.87–2.95)	0.0603	$3.37 \pm 0.01_c$ (3.34–3.41)	0.0448	$4.90 \pm 0.04_d$ (4.82–4.99)	0.0684

Note: different subscripts letter between columns and rows indicate statistically significant different values. ($\alpha = 0.05$).
[a] Values are expressed as best fit values for three replications ± standard error and (95% asymptotic confidence interval). RMSE = root mean square error.

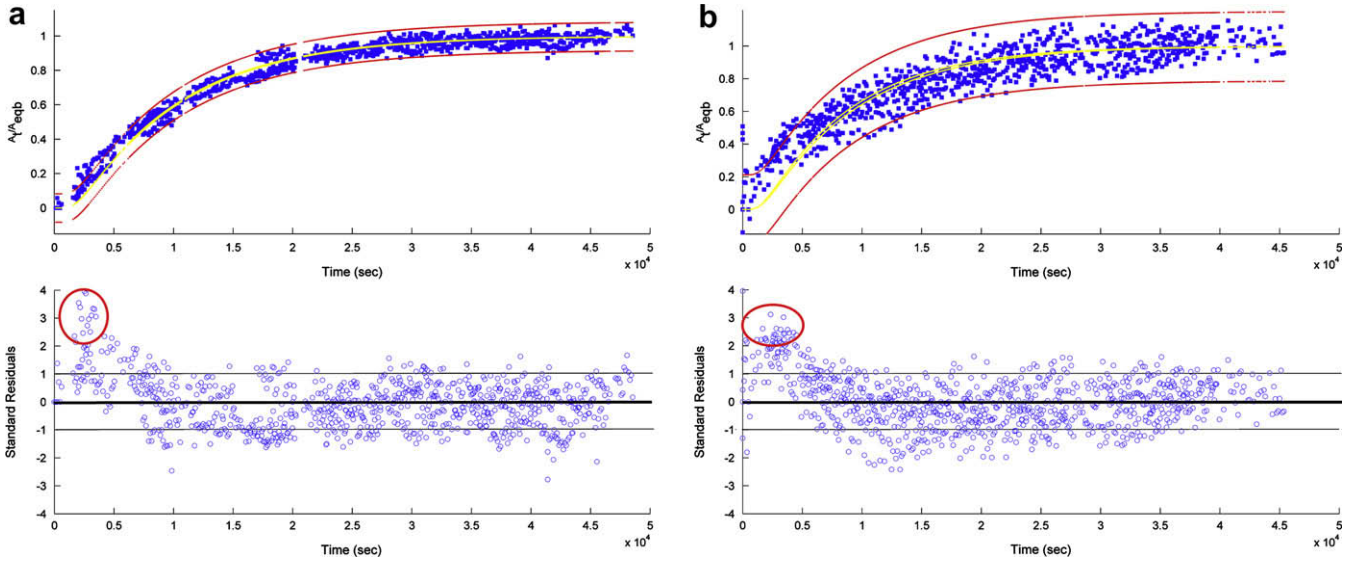

Fig. 7. FTIR-ATR normalized eugenol (1514 cm^{-1}) absorbance vs time for 23 °C at two depth of penetration (a) $d_p = 1.25$ μm, $\theta = 45°$ and (b) $d_p = 3.34$ μm, $\theta = 39°$. The central line shows the best fit to the dotted experimental values of all the three replications. The outer lines show the prediction interval for the observed experimental values. The confidence interval of the best fit is very close to the fitted curve and not clearly visible in figure (a) but visible in case of figure (b) due to higher variation in data. The standard residuals are shown in the graphs below with dark line indicating zero residual. The red oval indicates the higher residuals. (For interpretation of the references to colour in this figure legend, the reader is referred to the web version of this article.)

sided HPLC based diffusion process respectively. The insets in the figures show the normalized mass gain at short times or unsteady state of diffusion process. It can be seen that experimental values exhibit Fickian behavior. The central line passing through experimental values is the best-fit diffusion curve obtained by using Equation (11). The inner lines around the best-fit curve indicate its 95% confidence interval. The outer lines indicate the 95% prediction interval of the observed values. The errors in the HPLC data were within two standard residual values, so good fit of the experimental and predicted values could be established (Data not shown). It was also found that the D value in HPLC experiments was most sensitive (highest point of sensitivity curve) in the region $0.5 < M_t/M_{eqb} < 0.8$ (Data not shown).

As shown in Figs. 8a, 10a and 11a that the equilibrium time in case of two-sided HPLC (1×10^4 s or 2.8 h at 16 °C) and one-sided HPLC (3×10^4 s or 8.3 h at 16 °C) method was much shorter compared to FTIR-ATR method (10×10^4 s or 28 h at 16 °C). The difference in the equilibrium time in the two-sided and one-sided HPLC experiments was evidently due to the faster sorption of eugenol from the two surfaces of LLDPE exposed in the former compared to one side in the latter process. But the difference in equilibrium time between FTIR-ATR process and one-sided HPLC process was not only due to slower diffusion observed in former process but also contributed by the lag time (approximately zero absorbance till 0.5×10^4 s or 1.4 h in Fig. 8a) This lag time is due to the time required for eugenol to diffuse through the film and come in range of the evanescent field ($d_p = 1.25$ μm), where it can be detected. Table 4 summarizes the FTIR-ATR and HPLC double and single sided results at three temperatures. The D values for two-sided and one-sided HPLC are statistically not significantly different ($p = 0.05$). The FTIR-ATR values are statistically different compared to both single side and two side diffusion process. Eugenol D values have been reported to vary in high to low density polyethylene (HDPE to LDPE) at 23 °C from 1.3 to 10×10^{-10} cm^2/s [42]. However these values were calculated with the polymer phase in contact with a methanol/ethanol liquid phase. This contact with the organic liquids may have actually accelerated the loss of eugenol from the film, thereby driving the diffusion coefficient to higher values. On the other hand, a more recent study by Vitrac et al., used the molecular descriptors like Van-der-Waal volume, gyration radius and a dimensionless shape parameter in the process of decision tree to estimate D values of various compounds in polyolefins [43]. By this technique, the D value of eugenol was estimated to be 1.25×10^{-10} cm^2/s. To understand the significance of eugenol D values and as comparison with other organic compounds, diffusion of amyl acetate in HDPE showed a D value of 3.05×10^{-9} cm^2/s at 33 °C (by FTIR-ATR technique) [8], and butylated hydroxyl toluene (BHT) (I-1076) showed D value 2.2×10^{-9} cm^2/s at 50 °C [44]. Cava et al. used FTIR based desorption technique to find the D values of limonene (18.5×10^{-9} cm^2/s), linalool (3.8×10^{-9} cm^2/s), pinene (9.6×10^{-9} cm^2/s) and citral (5.5×10^{-9} cm^2/s) in polyethylene at 22 °C [45]. All these values were almost one order of magnitude higher than D of eugenol in LLDPE which could be expected of the higher volatility (higher partial pressure) than eugenol at the tested temperatures.

The activation energy of diffusion (E_D) was calculated by the two methodologies by fitting the Arrhenius equation (Equation (13)). Activation energy can be defined as the energy required by the permeant molecule to jump across the polymer chains by creating an opening between the chains [44].

$$D = D_0 \exp(-E_D/RT) \tag{13}$$

where D_0 is the pre-exponential factor (cm^2/s), R (8.314 kJ/K mol) is the gas constant and T is temperature (K). E_D values of 76.45, 74.95 and 74.68 kJ/mol for the FTIR-ATR, two-sided HPLC, and one-sided

Table 3
Diffusion coefficient (D) by FTIR-ATR at 45° and 39° incident angle and at 23 °C.

45°		39°	
$D \times 10^{-10}$ [a] (cm^2/s)	RMSE	$D \times 10^{-10}$ [a] (cm^2/s)	RMSE
$3.37 \pm 0.01_a$ (3.34–3.41)	0.0448	$4.10 \pm 0.06_b$ (3.98–4.23)	0.1278

Note: different subscripts letter between columns and rows indicate statistically significant different values. ($\alpha = 0.05$).

[a] Values are expressed as best fit values for three replications ± standard error and (95% asymptotic confidence interval). RMSE = root mean square error.

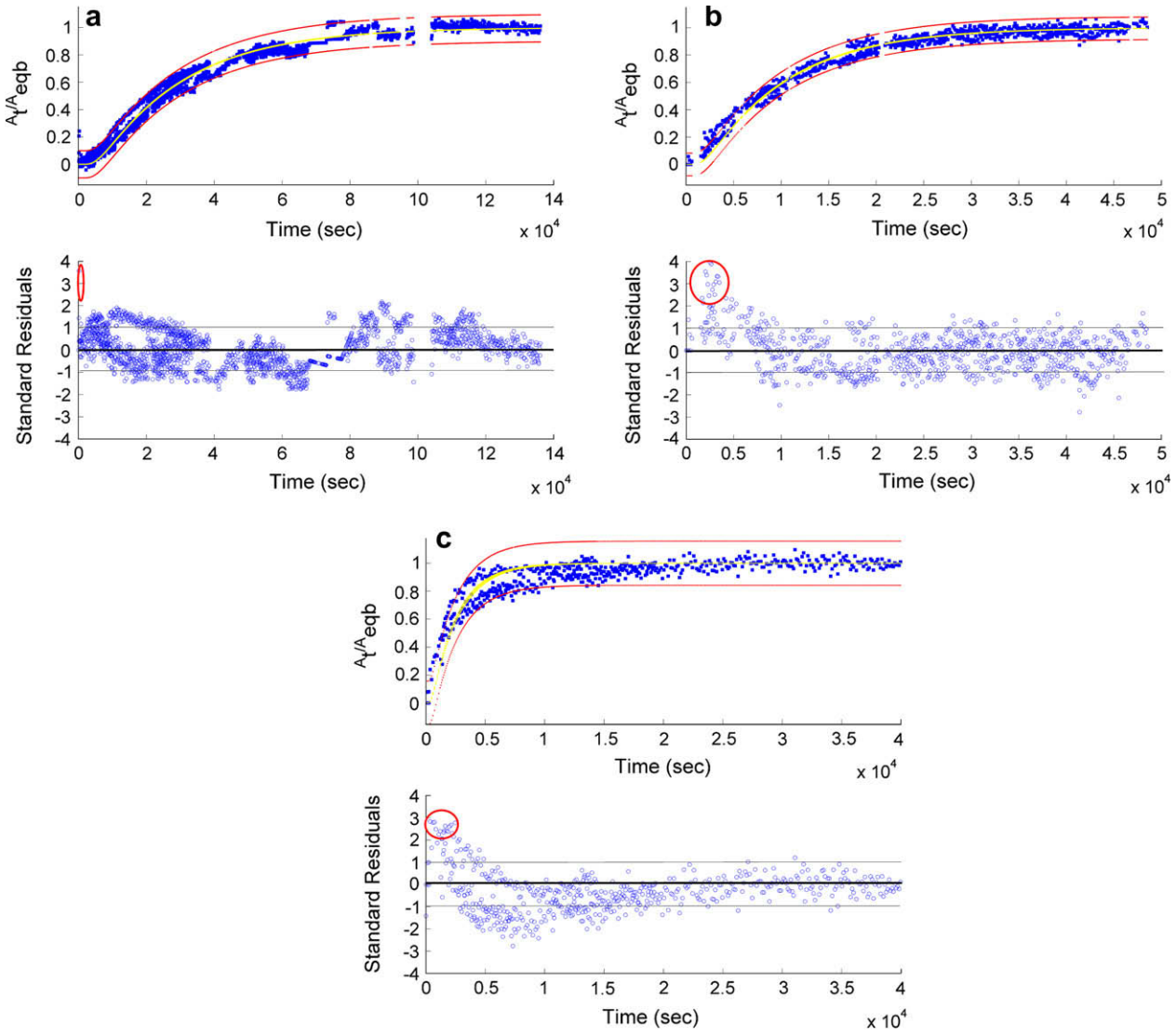

Fig. 8. FTIR-ATR normalized eugenol (1514 cm^{-1}) absorbance vs time for (a) 16 °C, (b) 23 °C and (c) 40 °C. The central line shows the best fit to the dotted experimental values of all the three replications. The outer lines show the prediction interval for the observed experimental values. The confidence interval of the best fit is very close to the fitted curve and not clearly visible in the figures. The standard residuals are shown in the graphs below with dark line indicating zero residual. The red oval indicates the higher residuals. (For interpretation of the references to colour in this figure legend, the reader is referred to the web version of this article.)

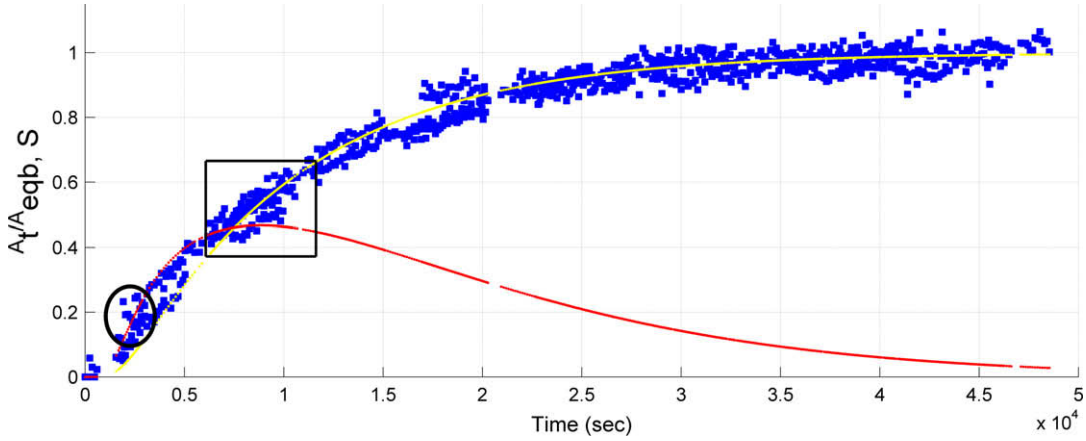

Fig. 9. FTIR-ATR normalized eugenol (1514 cm^{-1}) absorbance vs time for 23 °C. The central line shows the best fit to the dotted experimental values of all the three replications. The dotted points i.e. Sensitivity S vs time is overlapped on ATR values and ATR best fit. The dark oval indicates the initial residuals, while the square indicates the data points in region of highest S. Note: The sensitivity S and A_t/A_{eqb} have same scale.

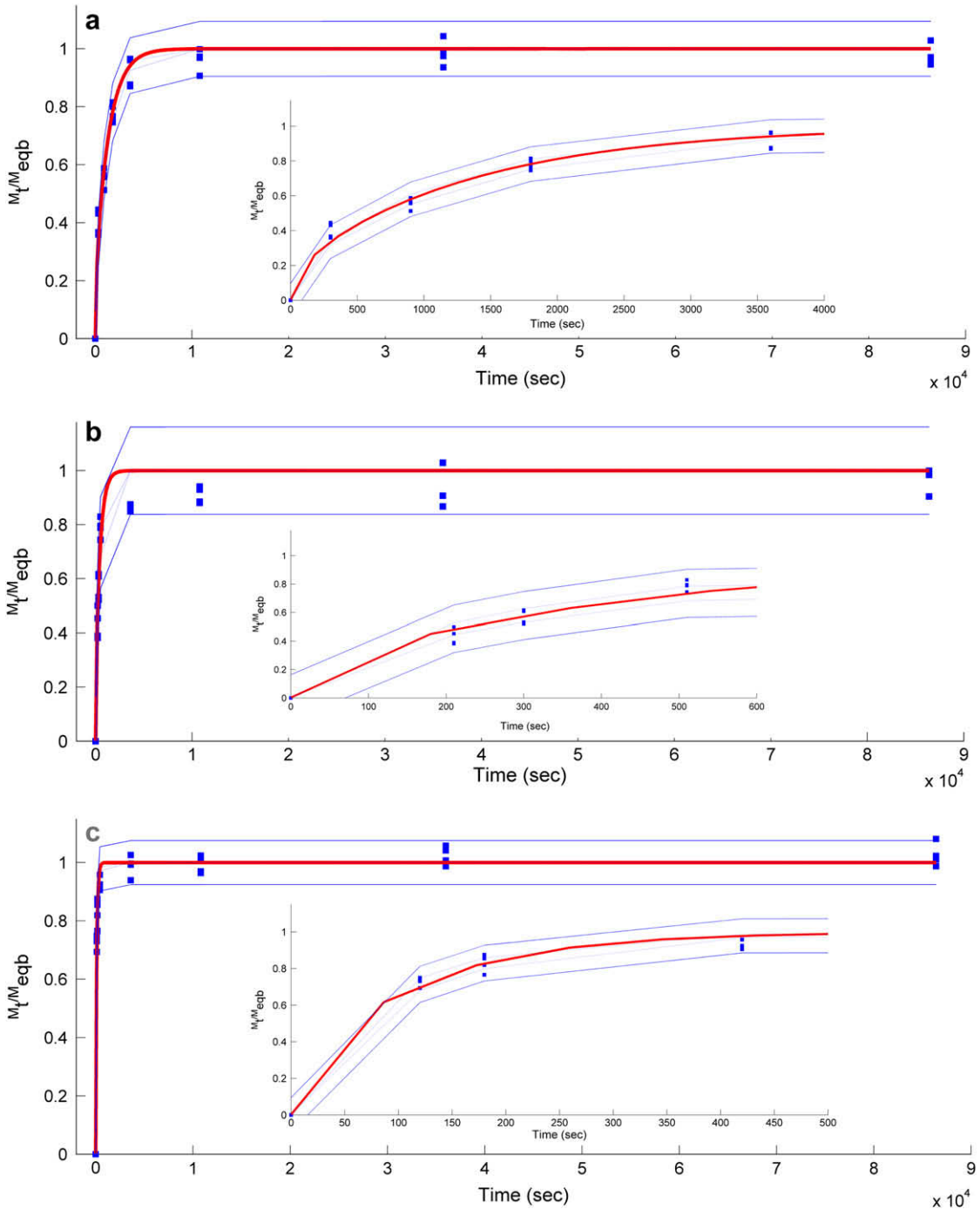

Fig. 10. HPLC two-sided normalized eugenol mass gain vs time at (a) 16 °C, (b) 23 °C and (c) 40 °C. The central line shows the best fit to the dotted experimental values. The outer lines show the prediction interval for the observed experimental values. The inner lines around the best-fit curve are the confidence intervals for the best fit. Note: The best-fit curve appears to deviate from 95% CI at some points away from experimental values because of the ways both are obtained. The prediction and confidence interval points are obtained at times where experimental data is present and then joined to form a curve. Hence they are not smooth. The best-fit curve, on other hand, was obtained by obtaining first the best *D* value and then finding the normalized mass gain in Equation (11) with this *D* value and using time intervals much smaller than the actual experimental time intervals. This resulted in smooth fitting curve.

HPLC, were obtained, respectively (Table 5). Activation energy of some saturated hydrocarbons such as n-hexane and n-decane through low density poly(ethylene) (LDPE) film has been reported. E_D depends on penetrant size and shape and seems to increase with n-hexane having a value 67.7 kJ/mol to n-decane having 96.8 kJ/mol [46]. E_D value of toluene diffusion in LDPE was reported to be 87 kJ/mol [47]. Antioxidants like methylester and octadecylester – Irganox 1076 had E_D values of 87 and 104 kJ/mol in LDPE [48].

The *D* values were of the same order of magnitude in all the three different experiments for all three temperatures. But the higher value of *D* for two-sided and one-sided HPLC compared to FTIR-ATR based value is not well understood and may be due to the inherent difference in the two measuring techniques. *D* value of 8.86×10^{-10} and 8.46×10^{-10} cm^2/s was observed for two-sided and one-sided HPLC based diffusion process respectively, as against 3.37×10^{-10} cm^2/s obtained in ATR result at 23 °C. Higher values of

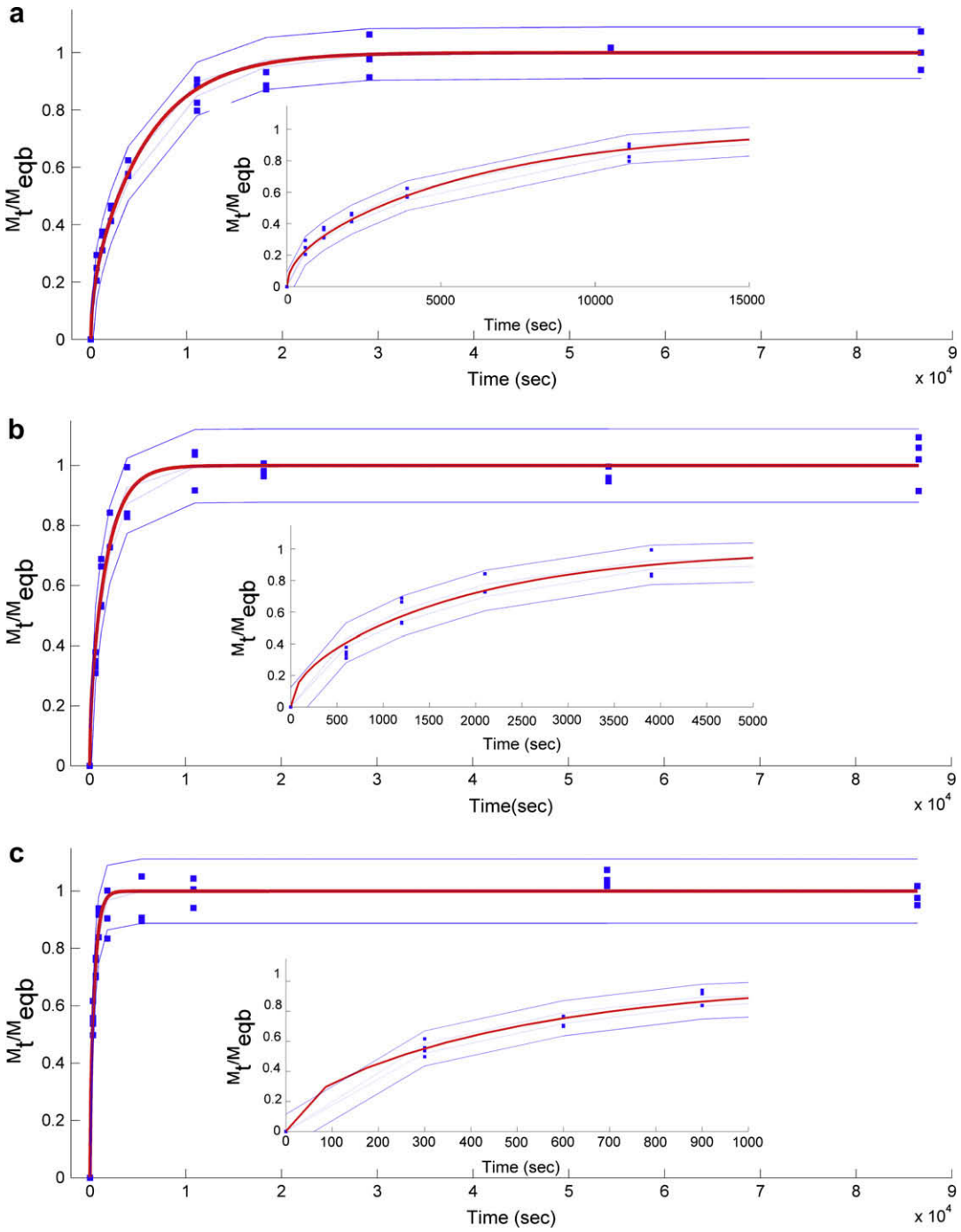

Fig. 11. HPLC one-sided normalized eugenol mass gain vs time at (a) 16 °C, (b) 23 °C and (c) 40 °C. The central line shows the best fit to the dotted experimental values. The outer lines show the prediction interval for the observed experimental values. The inner lines around the best-fit curve are the confidence intervals for the best fit.

Table 4
Diffusion coefficient (D) by FTR-ATR and HPLC techniques.

Temperature, °C	FTIR-ATR		HPLC two-sided		HPLC one-sided	
	$D \times 10^{-10}$ [a] (cm^2/s)	RMSE	$D \times 10^{-10}$ [a] (cm^2/s)	RMSE	$D \times 10^{-10}$ [a] (cm^2/s)	RMSE
16	$1.05 \pm 0.01_a$ (1.05–1.07)	0.0683	$2.96 \pm 0.15_b$ (2.66–3.27)	0.0463	$2.71 \pm 0.13_b$ (2.43–2.99)	0.0440
23	$3.37 \pm 0.01_c$ (3.34–3.41)	0.0448	$8.86 \pm 0.69_d$ (7.44–10.28)	0.0741	$8.46 \pm 0.60_d$ (7.23–9.69)	0.0663
40	$13.23 \pm 0.18_e$ (12.86–13.61)	0.0631	$35.11 \pm 1.60_f$ (31.85–38.37)	0.0370	$32.19 \pm 1.87_f$ (28.41–35.99)	0.0545

Note: different subscripts letter between columns and rows indicate statistically significant different values. ($\alpha = 0.05$).
[a] Values are expressed as best fit values for three replications ± standard error and (95% asymptotic confidence interval). RMSE = root mean square error.

Table 5
Activation energy (E_D) by FTR-ATR and HPLC techniques.

	FTIR-ATR	HPLC two-sided	HPLC one-sided
E_D (kJ/mol)	76.45	74.95	74.68
D_o (cm^2/s)	8216.50	12112.58	10084.96
R^2	0.9707	0.9769	0.9707

D in case of amyl acetate sorption in LDPE by gravimetric measurement using saturated vapor compared to FTIR-ATR results with liquid have also been reported by Balik et al. [8]. A possible source of error leading to higher D values in HPLC based results could be the inability to efficiently clean eugenol from the polymer surface, resulting in higher concentrations than those in the film. Additional steps like weighing of the film and extraction may contribute to the higher error seen in HPLC based values. It is also evident that it is not possible to continuously monitor the entire diffusion process in the HPLC (also known "pat and dry") as in FTIR-ATR technique, especially at higher temperatures. A possible error involved in eugenol absorbance change may be due to the measurement error in $A_{t=0}$. $A_{t=0}$ was the IR absorbance value measured as soon as eugenol was in contact with the LLDPE film (eugenol could be seen entering and exiting the flow cell through small glass tube at inlet and outlet of flow cell). But this absorbance value was obtained after performing 35 scans, which meant that eugenol was already in contact for ~1 min. Another source of error in $A_{t=0}$ is that the LLDPE film and crystal contact would not have been stable when eugenol had just entered the cell. This was evident from the fact that air bubbles were observed exiting the glass tube at the outlet of the flow cell when the IR measurement scans had started. So, if the actual $A_{t=0}$ value is lower than that which is expected to have been obtained if the contact was perfect, it may be responsible for higher residual in the initial phase until the contact became stable. A similar problem of polymer film/crystal contact stability has been discussed by Yi et al. [28], who have also suggested a mathematical correction applicable in cases where peak ratioing is performed.

In FTIR-ATR technique, monitoring of the spectrum throughout the diffusion process did not indicate any anomalous changes like wavelength shift [10] in absorbance peaks, indicating that there was no polymer penetrant interaction. Also, though the LLDPE peaks were overlapped by eugenol peaks, we did not observe any slow or abrupt decrease in LLDPE absorbance at any stage in the diffusion process, indicating that there was no significant swelling in the film. Fig. 12 shows the increase in the OH stretching bond (Table 1) absorbance as the diffusion proceeds. The larger arrow shows the direction of increase in absorbance of OH stretching bond with time, for the entire diffusion process. The smaller arrow indicates higher relative increase of the 3520 cm^{-1} region of the OH peak towards the end of the process, which may be due to the formation of eugenol clusters in the polymer film or due to the contact of eugenol with the ATR crystal, as the film gets saturated.

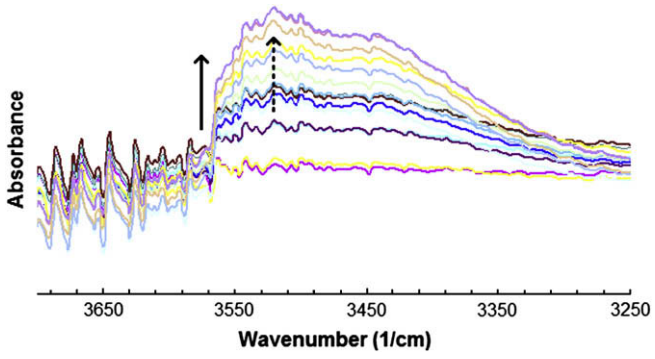

Fig. 12. Absorbance of OH stretching bond in eugenol.

5. Conclusion

An FTIR-ATR flow cell setup was successfully used to find the diffusion coefficient of eugenol through LLDPE film. Eugenol diffusion coefficients through LLDPE were found to be in the range of 1.05 ± 0.01 and $13.23 \pm 0.18 \times 10^{-10}$ cm^2/s through the temperature range tested (16–40 °C). The diffusion coefficients found by HPLC technique compared favorably with the FTIR-ATR results since they were in the same order of magnitude but actually higher. One and two-sided HPLC diffusion values between 2.71 ± 0.13 and $35.11 \pm 1.60 \times 10^{-10}$ cm^2/s at the same temperature range were determined. Activation energies, 76.45, 74.95 and 74.68 kJ/mol for the FTIR-ATR, HPLC two-sided, and HPLC one-sided respectively were calculated for eugenol diffusion through LLDPE. Unlike HPLC, ATR method helps monitor the entire diffusion process and requires less time to set up and to determine the diffusion coefficient values. Hence, FTIR-ATR technique can also be used in permeant/polymer systems where peak ratioing is not possible.

Complex organic compounds like eugenol, that are derived from plant extracts show great potential as natural antimicrobials and antioxidants [34]. Such extracts can be incorporated in polymer films and their migration in the food matrix may allow prolonging the shelf life. However, these active compounds may interact with the polymers, causing a change in their physical or chemical properties. It is necessary to study these changes. Hence, FTIR-ATR technique shows good potential to study the diffusion analysis and hence release of such compounds through polymer films.

Acknowledgement

The authors would like to thank the Center for Food and Pharmaceutical Packaging Research (CFPPR) from the School of Packaging, MSU for partially funding this project, and Dharmendra Mishra for helping with the Matlab code development.

References

[1] Hernandez RJ, Gavara R. Plastics packaging: methods for studying mass transfer interactions. Pira International 1999.
[2] Pawlisch CA, Macris A, Laurence RL. Macromolecules 1987;20:1564–78.
[3] Koptyug IV, Sagdeev RZ. Russian Chemical Reviews 2002;71(10):789–835.
[4] Leewis CM, Mutsaers PHA, de-Jong AM, van-IJzendoorn LJ, Broer DJ, de Voigt MJA. Nuclear Instruments and Methods in Physics Research 2001;B181:367–71.
[5] Cava D, Catala R, Gavara R, Lagaron JM. Polymer Testing 2005;24:483–9.
[6] Bobiak JP, Koenig JL. Journal of Controlled Release 2005;106:329–38.
[7] Fleming OS, Andrew Chan KL, Kazarian SG. Polymer 2006;47:4649–58.
[8] Balik CM, Simendinger III WH. Polymer 1998;39:4723–8.
[9] Doopers LM, Sammon C, Breen C, Yarwood J. Polymer 2006;47:2714–22.
[10] Elabd YA, Baschetti M, Barbari TA. Journal of Polymer Science 2003;41:2794–807.
[11] Esmaiel J, Peppas NA. Macromolecules 1993;26:2175–86.
[12] Farinas KC, Doh L, Venkatraman S, Potts R. Macromolecules 1994;27:5220–2.
[13] Fieldson GT, Barbari TA. American Institute for Chemical Engineering Journal 1995;41:795–804.
[14] Fieldson GT, Barbari TA. Polymer 1993;34(6):1146–53.
[15] Hanh BD, Neubert RHH, Wartewig S. International Journal of Pharmaceutics 2000;204:145–50.
[16] Hellstern U, Hoffmann V. Journal of Molecular Structure 1995;349:329–32.
[17] Laity PR, Hay JN. Cellulose 2000;7:387–97.
[18] Morrissey P, Vesely D. Polymer 2000;41:1865–72.
[19] Mountz DA, Storey RF, Mauritz KA. Journal of Polymer Science 2005;43:764–76.
[20] Murphy B, Kirwan P, McLoughlin P. Analytical and Bioanalytical Chemistry 2003;377:195–202.
[21] Murphy B, Kirwan P, McLoughlin P. Vibrational Spectroscopy 2003;33:75–82.
[22] Persson D, Ohmana M, Leygraf C. Progress in Organic Coatings 2006;57:78–88.

[23] Pereira AM, Lopes MC, Timmera JMK, Keurentjes JTF. Journal of Membrane Science 2005;260:174–80.
[24] Philippe L, Sammon C, Lyon SB, Yarwood J. Progress in Organic Coatings 2004;49:302–14.
[25] Schmidt P, Dybal J, Trchova M. Vibrational Spectroscopy 2006;42:278–83.
[26] Hajatdoost S, Sammon C, Yarwood J. Polymer 2002;43:1821–7.
[27] Hace I, Golob J, Krajnc M. Chemical and Biochemical Engineering 2004; 18(1):73–6.
[28] Yi X, Portnoy J, Pellegrino J. Journal of Polymer Science, Part B: Polymer Physics 2000;38:1773–87.
[29] Uda Y, Kaneko F, Kawaguchi T. Polymer 2004;45:2221–9.
[30] Jen JF, Liu TC. Journal of Chromatography 2006;1130:28–33.
[31] Silva AS, Cruz Freire JM, Franz R, Losada PP. Food Research International 2008;41:138–44.
[32] Valero M, Salmeron MC. International Journal of Food Microbiology 2003;85:73–81.
[33] Remmal A, Khadija R, Bouchikhi T, Tantaoui-Elaraki A, Sendide K. Journal of Essential Oil Research 2003;15:356–62.
[34] Holley RA, Patel D. Food Microbiology 2005;22:273–92.
[35] Mirabella FM, editor. Internal reflection spectroscopy, theory and applications. Marcel Dekker; 1992.
[36] Huang JB, Hong JW, Urban MW. Polymer 1992;33:5173–8.
[37] Mirabella Jr FM. Journal of Polymer Science: Polymer Physics Edition 1983;21:2403–17.
[38] Crank J. The mathematics of diffusion. New York: Oxford University Press; 1975.
[39] Freund RJ, Wilson WJ. Statistical methods. Academic Press, 2003.
[40] Beck JV, Arnold KJ. Parameter estimation in engineering and science. New York: John Wiley & Sons; 1977.
[41] Yasuda H, Peterlin A. Journal of Applied Polymer Science 1973;17:433–42.
[42] Piringer O-G, Baner AL, editors. Plastic packaging materials for food. Weinheim: Wiley-VCH; 2000.
[43] Vitrac O, Lezervant J, Feigenbaum A. Journal of Applied Polymer Science 2006;101:2167–86.
[44] Limm W, Hollifield HC. Food Additives and Contaminants 1995;13(8):949–67.
[45] Cava D, Lagaron JM, Lopez-Rubio A, Catala R, Gavara R. Polymer Testing 2004;23:551–7.
[46] Asfour AA, Saleem M, DeKee D, Harrison B. Journal of Applied Polymer Science 2003;38(8):1503–14.
[47] Saleem M, Asfour AA, DeKee D, Harrison B. Journal of Applied Polymer Science 2003;37(3):617–25.
[48] Moller K, Gevert T. Journal of Applied Polymer Science 1993;51:895–903.